DESIGN AND ANALYSIS OF AXIAL-FLUX CORELESS PERMANENT MAGNET DISK GENERATOR

Łukasz DRĄZIKOWSKI Włodzimierz KOCZARA

Institute of Control and Industrial Electronics
Warsaw University of Technology, Warsaw, Poland
e-mail: drazikol@ee.pw.edu.pl, koczara@isep.pw.edu.pl

Abstract: *Magnets are an important part of modern electric machines. Thanks to them motors become lighter and reliable because of brushless technology. This article presents simple and easy to manufacture design of permanent magnet generator based on coreless windings. This axial-flux machine seems to be very interesting for low speed power generation systems such as wind and water turbines. There is also shown an example of basic calculations based on equivalent magnetic circuit. The analysis presents flux dependence on several parameters such as: magnet's grade and size in comparison with coil and air-gap dimensions. Second part of the article concentrates on simulation results of Finite Element Method analysis (FEM) that clearly shows the flux distribution for different magnet shapes – trapezoidal and rectangular. Finally there is presented a description of a 20kW prototype of PMSG based on rectangular magnets which contains mechanical design and a experimental results.*

Keywords: Permanent magnet, FEM, disk generator, coreless, ironless, air-core, axial-flux, PMSM, PMSG, AFPM, air-gap, magnetic circuit, coil, windings, rotor.

1. Introduction

In electric generators magnets function as transducers, transforming mechanical energy to electrical energy without any permanent loss of their own energy. That means the better magnet the better transducer and finally the better whole device. That is why, it is so important to learn basics of magnets before designing the machine. Nowadays, Neodymium Iron Boron (NdFeB) magnets are widely known as the best one [1][2]. This modern magnetic material is easily available on the market in different grades and shapes. Thanks to them high efficiency electric machines can be designed. Permanent magnet electric generators are needed in renewable energy sources. They can provide power even during electrical network failure because of built-in permanent self-excitation.

2. Parameters of neodymium magnets

Magnetic material can be described by the *B(H)* curve. Second quadrant of this characteristic is called demagnetization curve and is useful for magnetic calculation. The point where this characteristic cross *H* axis is called Coercivity (H_c) which is a value of external magnetic field required to reduce magnetization of this material to zero. Second important parameter is remanence (B_r) which is residual flux density *B*. Value of B_r tells about the magnetization of material when external magnetic field (*H*) is removed. Being based on those two components it is possible to determine demagnetization curve. This function is almost linear for neodymium magnets and can be approximate by the equation (1).

$$B(H) = \frac{B_r}{H_c} H + B_r \qquad (1)$$

Having this equation it is easy to determine a maximum energy product $(BH)_{max}$. This parameter of permanent magnet is used by the manufacturers to specify the grade of the magnet and can be calculated by the equation (2).

$$(BH)_{\max} = 0{,}25 \cdot B_r H_c \qquad (2)$$

The higher energy density the smaller volume of magnet is needed to obtain the same flux density in the air-gap. Grade of permanent magnet is often shown in CGS (Centimeter-Gram-Second) system of units (MGOe) and it functions on the market as a symbol of N (e.g. N45). Units conversion factors are presented in table (1).

Table 1: Units conversion factors.

System of units	CGS	SI
Flux density	1 Gs	10^{-4} T
Magnetic field	1 Oe	$\frac{1}{4\pi \cdot 10^{-3}} \approx 79{,}58$ A/m
Energy density (grade)	1 MGOe	$\frac{1}{4\pi \cdot 10^{-2}} \approx 7{,}96$ kJ/m^3

3. Machine topology and mechanical design of magnetic circuit

Presented device is a 12 pair poles synchronous machine. Double rotor is equipped with 24 magnets per disk. Air-core three phase windings are placed between magnets (Fig. 2). This topology has several advantages, e.g. there is no starting and cogging torque what is very important especially for wind power systems. Moreover, it is cheap, easy to manufacture, and can be produced in the range of single watts up to hundreds of kilo watts of power in multi disk operation [1][2][3][4][5].

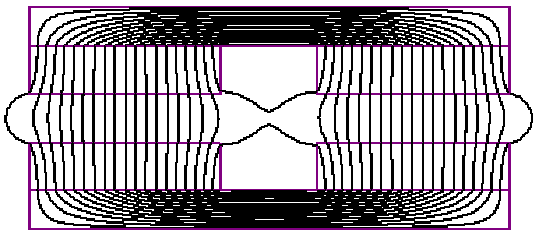

Figure 1: Simplified magnetic circuit.

It is resistant for short time overload because of air-core which is free of saturation. The biggest drawback is a need of use stronger magnets to obtain the same power like in conventional iron-core machine which is the reason of higher reluctance of magnetic circuit. Besides some sensorless control methods cannot be applied in this topology [6]. For analytical discussion, magnetic circuit of this machine can be simplified to four magnets – two on first rotor disk and other two on the second disk. That is shown in the picture (1).

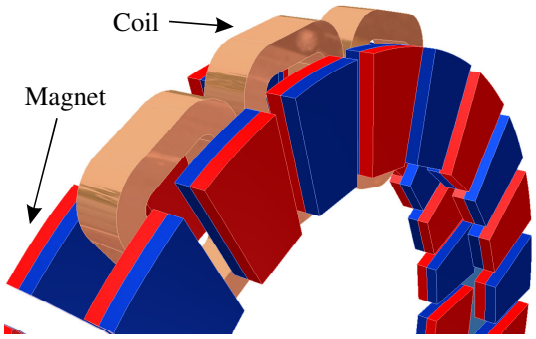

Figure 2: Isometric view of mechanical topology.

4. Analytical calculations based on equivalent magnetic circuit

Magnetic circuits are very similar to electric circuits, so it is possible to use the same analytical equations for both. Especially, in presented case, where the core is free of iron, this transformation is proper for whole range of magnetic fields. Analytical modeling is enough to calculate approximated flux density in the air-gap, which is the base of father voltage and power calculations. Equivalent magnetic circuit (Fig. 3) can be described by following equation (3).

$$B_m = \frac{\phi}{S} = \frac{\Theta}{S \cdot R_m} = \frac{2\Theta_{PM}}{S \cdot (R_{AG} + 2R_{PM})} \qquad (3)$$

where: B_m – maximum of flux density in the air-gap, ϕ – the flux that goes through the area S, R_{AG} and R_{PM} – the reluctances of air-gap and permanent magnet, Θ – total magnetomotive force.

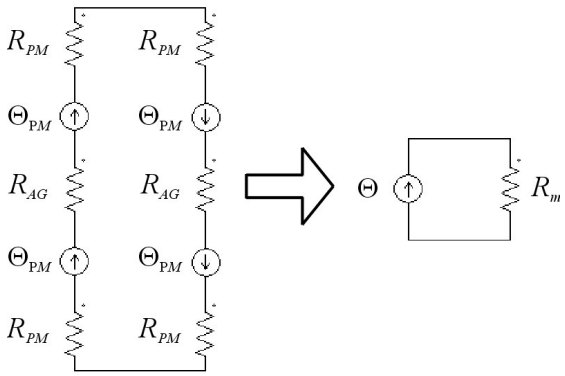

Figure 3: Equivalent magnetic circuit.

Magnetomotive force depends on two parameters – magnet thickness g and magnet coercivity H_c. It is given by formula (4).

$$\Theta_{PM} = g \cdot H_c \qquad (4)$$

Reluctance of material can be easily calculated by equation (5). Value of reluctance depends on material permeability μ and its dimensions – length l and area S that flux is going through.

$$R = \frac{l}{\mu \cdot S} \qquad (5)$$

Finally the maximum flux density between magnets is described by the expression (6), where μ_0 is air permeability that equals $4\pi \cdot 10^{-7} \frac{H}{m}$ and δ is air-gap length.

$$B_m = \frac{2g\mu_0 B_r H_c}{B_r \delta + 2g\mu_0 H_c} \qquad (6)$$

This is only approximated value of maximum flux density because of leakage flux which cannot be easily calculated. Leakage flux mainly depends on air-gap and magnets dimension. The worst case is when the air-gap length is high. In that case it can be assumed that flux density shape is sinusoidal. That means that flux distribution may be expressed as a function of sin(x) (7).

$$B(x) = B_m \sin\left(\frac{\pi}{\tau} x\right) \qquad (7)$$

Pole pitch τ is a distance between magnets placed on the same rotor disk. In presented topology pole pitch is a function of rotor radius r. There is 24 magnets on each disk so that means that angular pole pitch is 360°/24 = 15°. For analysis it is needed to have linear pole pitch in [mm] what can be calculated by following equation (8).

$$\tau = 2r \sin(7.5°) \qquad (8)$$

Calculations of electromotive force depend on coil dimensions. Because of coreless topology, wires are distributed along the air-gap. That means that every wire of the coil works in different conditions. Some of them are in the strong magnetic field while other are in the edge of magnet where the flux density is much lower. This must be taken into account while calculation EMF. The idea is to calculate average value of flux density at the area where the coil is. This can be expressed by integral equation (9).

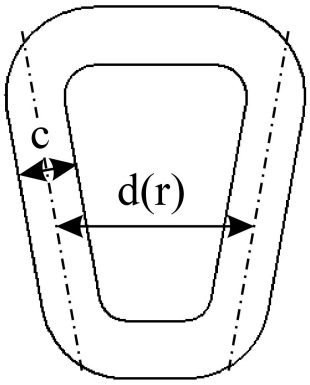

Figure 4: Coil dimensions.

$$E(x) = k\frac{2\pi r \cdot n}{60} lz \frac{1}{c}\left[\int_{x-1/2c}^{x+1/2c} B_m \sin\left(\frac{\pi}{\tau}x\right)dx - \int_{x-1/2c}^{x+1/2c} B_m \sin\left(\frac{\pi}{\tau}(x+d)\right)dx\right] \quad (9)$$

where:

k – number of coils per phase; r – radius; n – rotor rotation speed [rpm];
l – length of conducting wire; z – number of turns; c – coil thickness (Fig. 4);
d – coil diameter (Fig. 4); x – actual position [mm]; E – electromotive force.

5. Air gap size optimization

Equation (6) describes dependence between flux density and air-gap size. This relation is strongly nonlinear. Moreover, several other parameters must be taken into account while calculating output power of the machine. Increasing air-gap, value of flux density is falling down while number of turns is rising. That has an influence on total impedance. Relation between impedance and number of turns in also nonlinear, because inductance of the coil depends on the square of number of turns. In total output power as a function of air-gap has a maximum shown in figure (5).

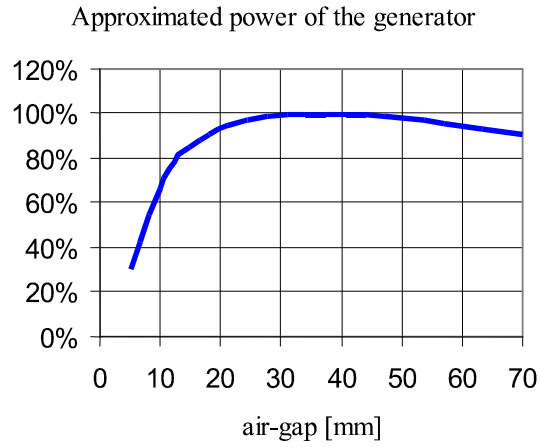

Figure 5: Approximated power of the generator.

For this machine optimum air-gap size is about 35 mm. Looking on this characteristic, it can be seen that the output power is almost constant between 33 and 38 mm of the air-gap. For economic reasons, the lower size has been chosen (33 mm) in the prototype, because increasing air-gap in this range has no significant influence on total output power.

6. Coil and magnet size optimization

Coil and magnet size optimization are based on geometrical analysis. For given number of pair poles, which is 12, it is easy to calculate linear pole pitch as a function of rotor radius (8). In similar way, diameter of coil (Fig. 4) can be calculated. In order to calculate, the best relation between pole pitch and coil diameter equation (9) can be used. It consists of the difference of two sinusoidal functions. This formula will reach maximum only if those two sinuses are shifted in 180°. It can be achieved when coil width d is equal to pole pitch τ. Second parameter of the coil is its thickness c shown in figure (4). In order to keep diameter of the coil equal to pole pitch, the thickness of the coil cannot be increase more than 33% of pole pitch because of geometrical relations. It must be taken into account that this is three-phase system, so the distance between coils must be equal 133% of the pole pitch.

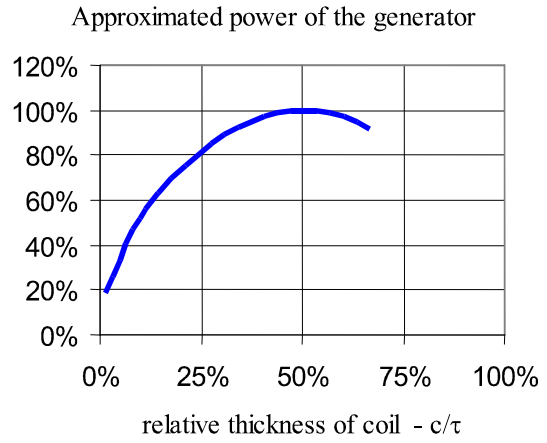

Figure 6: Approximated power of the generator.

Apparently in this case, there is not a maximum power (Fig. 6). It is possible to increase coil thickness to 50% of pole pitch while decreasing diameter from 100% to 83,3% of pole pitch. Decreasing of the diameter has a lower influence than increasing the number of turns. In total maximum power can be achieved in this case.
All those analysis have been made under assumption that the shape of flux density is sinusoidal. In order to increase maximum power, the width of the magnet can be also changed.

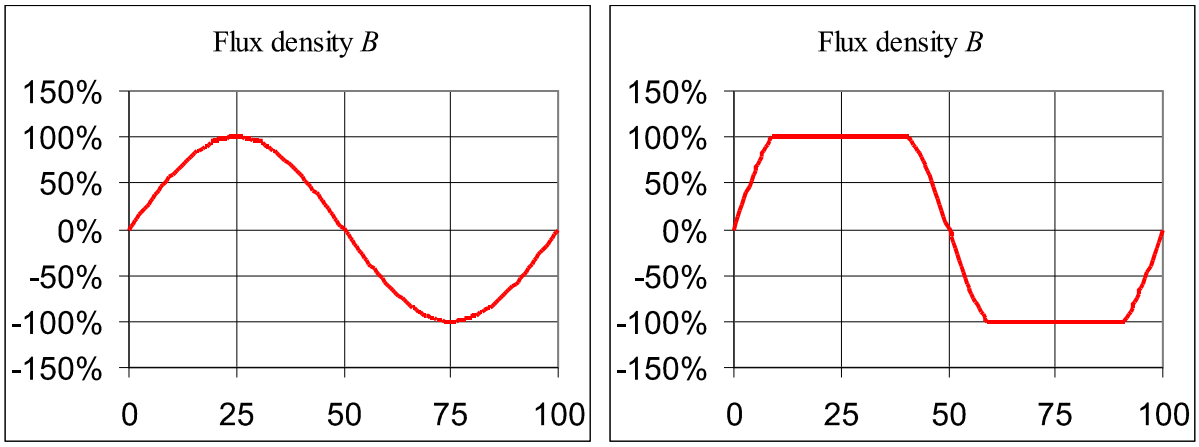

Figure 7: Comparison of flux densities.

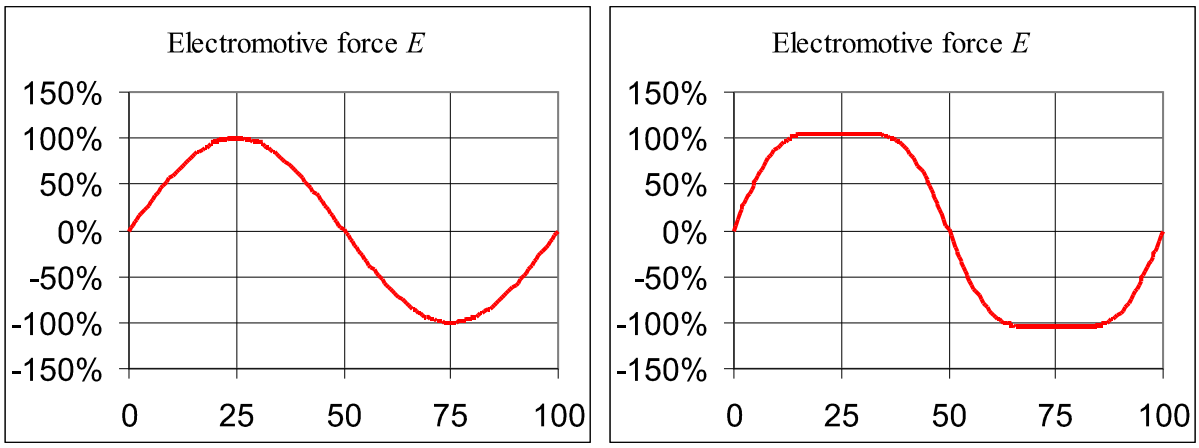

Figure 8: Comparison of line voltages.

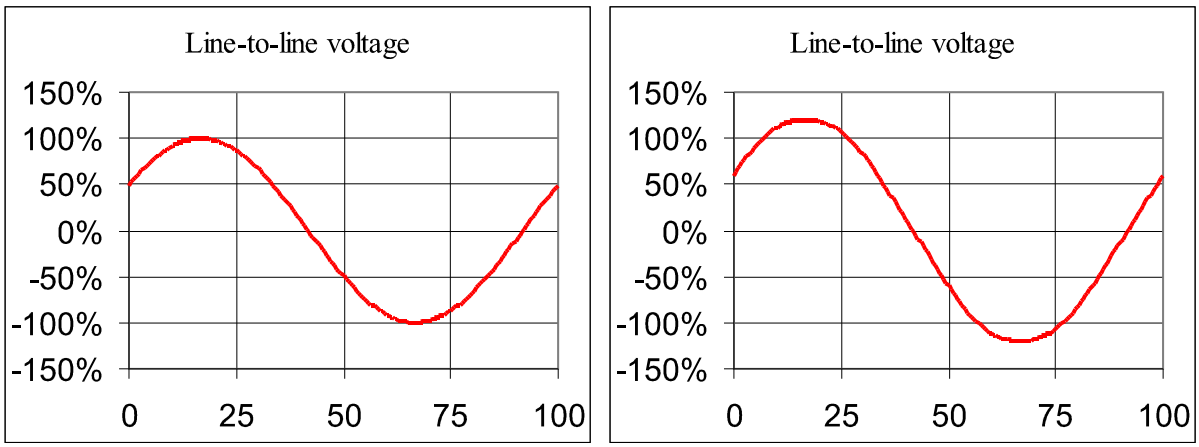

Figure 9: Comparison of line-to-line voltages.

The influence of widening the magnet on flux density shape cannot be easily calculated, but can be approximated. Maximum width of the magnet is equal to pole pitch. In that case, there is no free space between the magnets, so the shape of flux density should be more trapezoidal. Finite element

analysis and intuition says that the wider magnet the more trapezoidal shape of flux density. Pictures (7), (8), (9) are based on analytical calculations and they illustrate the phase voltage and line-to-line voltage for sinusoidal and trapezoidal flux density (Fig. 7). While widening the magnets, the third harmonic appears in line voltage (Fig. 8). The final result is that the total output voltage has been increased of 20% (Fig. 9).

7. Flux density analysis for different shapes of PM

Being based on the results of widening the magnet, next optimization step can be proposed. Considering that the linear pole pitch depends on the rotor radius (8) trapezoidal shape of the magnet can be applied in order to increase output voltage (Fig. 2).

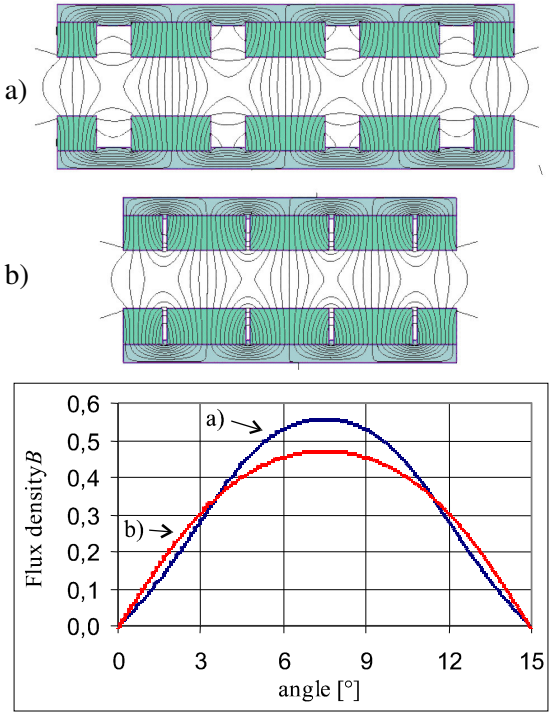

Figure 10: Flux density for different linear pole pitch

The simple two-dimensional finite element analysis has been made for different shapes of magnets. While widening magnet up to 100% of pole pitch some part of magnetic field is lost. To avoid this phenomenon free space between magnets should be designed. From FEM analysis follows that distance between two magnets should be equal to the thickness of the magnet (Fig. 10).

8. Experimental results

Presented topology of three-phase permanent magnet synchronous machine has been already implemented. All the mechanics has been designed in three-dimensional software. To achieve proper assembly of windings in order to keep very small air-gap between magnets and coils special tools and equipment has been designed and produced. Double disk rotor is equipped with double rolled spherical bearings to obtain long term life time.

Figure 11: Picture of PMSG.

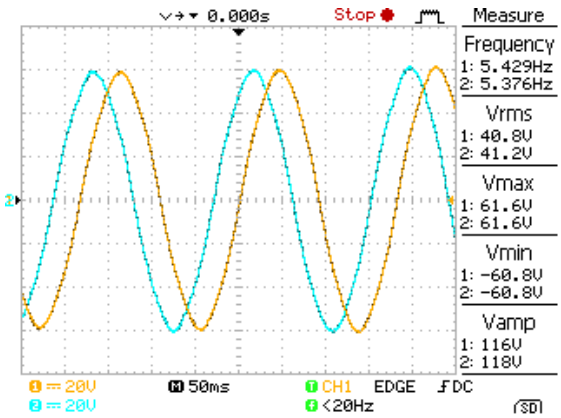

Figure 12: Line-to-line EMF.

Case of the machine has been cut out from the 10mm iron sheet and covered thin perforated aluminum sheet to obtain proper cooling (Fig. 11). Line-to-line voltage is a sinusoidal wave form with

only 1,6% of 5th harmonic (Fig. 12). Detailed specifications are shown below (Table 2).

Table 2: Specification of PMSG.

speed / frequency	**250 rpm / 50 Hz**
$U_{RMS\ line\text{-}to\text{-}line}$ unloaded / fully loaded	380 V / 353 V
$U_{RMS\ line}$ unloaded / fully loaded	220V / 204 V
$I_{RMS\ phase}$	15,0 A
Power	**9,1 kW**
Weight	190 kg
Dimensions	818/780/176 mm

In laboratory condition the load test has been done. There have been measured true RMS values of voltages and currents for different speeds. There was take into account only resistive load.

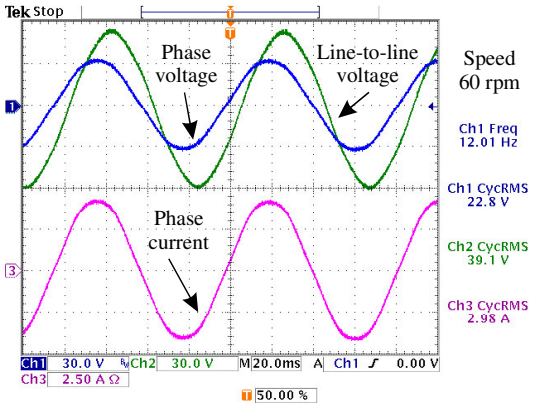

Figure 13: Example oscillograph of current and voltages during resistive load

Based on those oscillographs the output characteristic can be drawn. (Fig. 14) Generator has a strong output characteristic. The voltage drop is less that 8% during full load operation. Following figure presents output characteristic for speed range from 60 to 180 rpm.

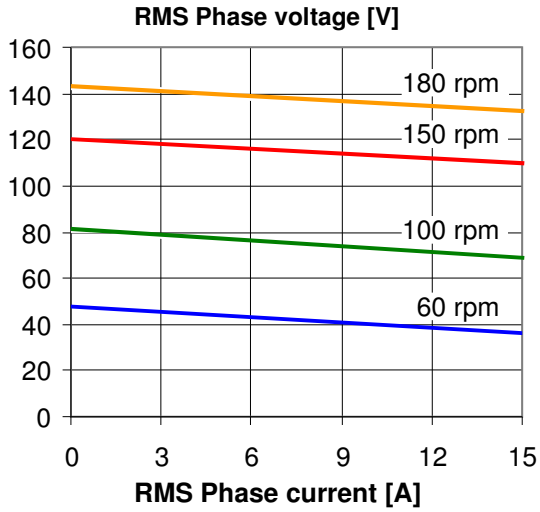

Figure 14: PMSG output characteristic

9. Conclusions

This paper has described the most important steps of designing magnetic circuit of coreless PMSM. Detailed analytical analysis has been made and two-dimensional FEM analysis has been applied in order to present flux distribution. The best size of the air-gap has been selected on the basis of output power calculation. The air-gap should be equal to 160% – 170% of the magnet thickness. Coil diameter and thickness has also been discussed. Flux distribution, which has been showed in FEM analysis, has told that the magnet cannot be widened up to 100% of pole pitch because of leakage flux. Trapezoidal magnet shape has been proposed in order to increase output voltage because of trapezoidal shape of flux density. Proper distance between magnets should be designed in this case. For verification, advanced prototype has been made. Machine has no cogging torque and starting torque is less than 2 Nm. Symmetrical three-phase windings provide constant torque at full range of power. Thanks to the coreless technology there is no hysteresis and eddy currents looses. That is why, achieved efficiency is 96% at 250 rpm and can be increased up to 98% at 600 rpm. During this operation machine can provide up to 20kW of active power. The last part of this paper describes experimental results. There is shown output characteristic of PMSG.

Acknowledgement

This work was financially supported by Institute of Control and Industrial Electronics, Warsaw University of Technology, Warsaw, Poland.

References

[1] S. Javadi and M. Mirsalim, "A Coreless Axial-Flux Permanent-Magnet Generator for Automotive Applications" in IEEE Transactions on Magnetics, Vol. 44, No. 12, pp. 4591-4598, December 2008

[2] T. F. Chan and L. L. Lai, "An Axial-Flux Permanent-Magnet Synchronous Generator for a Direct-Coupled Wind-Turbine System", in IEEE Transactions on Energy Conversion, Vol. 22, No. 1, pp. 86-94, March 2007

[3] P. Virtic, P. Pisek, T. Marcic, M. H. and B. Stumberger, "Analytical Analysis of Magnetic Field and Back Electromotive Force Calculation of an Axial-Flux Permanent Magnet Synchronous Generator With Coreless Stator", in IEEE Transactions on Magnetics, Vol. 44, No. 11, pp. 4333-4336, November 2008

[4] S. M. Hosseini, M. Agha-Mirsalim and M. Mirzaei, "Design, Prototyping, and Analysis of a Low Cost Axial-Flux Coreless Permanent-Magnet Generator", in IEEE Transactions on Magnetics, Vol. 44, No. 1, pp. 75-80 January 2008 75

[5] Chang-Chou Hwang, Ping-Lun Li, Frazier C. Chuang, Cheng-Tsung Liu, and Kuo-Hua Huang, "Optimization for Reduction of Torque Ripple in an Axial Flux Permanent Magnet Machine" in IEEE Transactions on Magnetics, Vol. 45, No. 3, pp. 1760-1763, March 2009

[6] J. Wiśniewski and W. Koczara, "Sensorless Control of Axial Flux Permanent Magnet Motor at Standstill and at Low Speed" in Electrical Review, 7/2009, pp. 177-181, July 2009